Loss of polyadenylation protein τCstF-64 causes spermatogenic defects and male infertility

Brinda Dass*, Steve Tardif*, Ji Yeon Park†, Bin Tian†, Harry M. Weitlauf*, Rex A. Hess‡, Kay Carnes‡, Michael D. Griswold§, Christopher L. Small§, and Clinton C. MacDonald*¶

*Department of Cell Biology and Biochemistry, Texas Tech University Health Sciences Center, Lubbock, TX 79430; ‡Department of Veterinary Biosciences, University of Illinois, Urbana, IL 61802; §Center for Reproductive Biology, School of Molecular Biosciences, Washington State University, Pullman, WA 99164; and †Department of Biochemistry and Molecular Biology, University of Medicine and Dentistry of New Jersey–New Jersey Medical School, Newark, NJ 07103

Polyadenylation, the process of eukaryotic mRNA 3′ end formation, is essential for gene expression and cell viability. Polyadenylation of male germ cell mRNAs is unusual, exhibiting increased alternative polyadenylation, decreased AAUAAA polyadenylation signal use, and reduced downstream sequence element dependence. CstF-64, the RNA-binding component of the cleavage stimulation factor (CstF), interacts with pre-mRNAs at sequences downstream of the cleavage site. In mammalian testes, meiotic XY-body formation causes suppression of X-linked CstF-64 expression during pachynema. Consequently, an autosomal paralog, τCstF-64 (gene name *Cstf2t*), is expressed during meiosis and subsequent haploid differentiation. Here we show that targeted disruption of *Cstf2t* in mice causes aberrant spermatogenesis, specifically disrupting meiotic and postmeiotic development, resulting in male infertility resembling oligoasthenoteratozoospermia. Furthermore, the *Cstf2t* mutant phenotype displays variable expressivity such that spermatozoa show a broad range of defects. The overall phenotype is consistent with a requirement for τCstF-64 in spermatogenesis as indicated by the significant changes in expression of thousands of genes in testes of *Cstf2t*−/− mice as measured by microarray. Our results indicate that, although the infertility in *Cstf2t*−/− males is due to low sperm count, multiple genes controlling many aspects of germ-cell development depend on τCstF-64 for their normal expression. Finally, these transgenic mice provide a model for the study of polyadenylation in an isolated *in vivo* system and highlight the role of a growing family of testis-expressed autosomal retroposed variants of X-linked genes.

spermatogenesis | oligoasthenoteratozoospemia | meiosis | XY body | meiotic sex chromosome inactivation

Fig. 1. Summary of defects in *Cstf2t*−/− mouse testes. Indicated is the timeline of mouse spermatogenesis (≈34 days), significant stages of spermatogenesis, and cell types in which CstF-64 (solid gray bar) and τCstF-64 (dashed box) proteins are expressed in wild-type mice. The first visible lesion in stage-XII secondary spermatocytes (arrow) and cumulative histological defects (step-10–16 spermatids, arrows and triangle) are indicated (see Fig. 3).

Polyadenylation, the process of mRNA 3′ end formation, is required for the synthesis, transport, translation, and stability of eukaryotic mRNAs (1, 2). Although polyadenylation is nearly universal, features of polyadenylation are different in mammalian male germ cells than in other tissues: male germ cell mRNAs exhibit increased alternative polyadenylation (3, 4), decreased use of the AAUAAA polyadenylation signal (5, 6), and reduced dependence on downstream sequence elements (DSEs) (7). These differences suggest a modified mechanism for polyadenylation in male germ cells.

While examining these differences, we discovered τCstF-64 (8), which is a paralog of the 64,000 M_r subunit of the cleavage stimulation factor (CstF-64) (9–11). CstF-64 is expressed in nuclei of early spermatogenic cells (5, 12). However, because it is on the X chromosome, CstF-64 expression halts in pachytene spermatocytes because of meiotic sex chromosome inactivation (MSCI) (13). In contrast, τCstF-64 expression begins in pachytene spermatocytes and continues in spermatocytes and early spermatids (refs. 5 and 12; summarized in Fig. 1). τCstF-64 is the only known CstF-64 homolog expressed during male meiosis, thus making it a candidate to play a critical role in spermatogenesis and male fertility. We hypothesize that τCstF-64 is necessary for spermatogenesis because it controls gene expression during germ cell development.
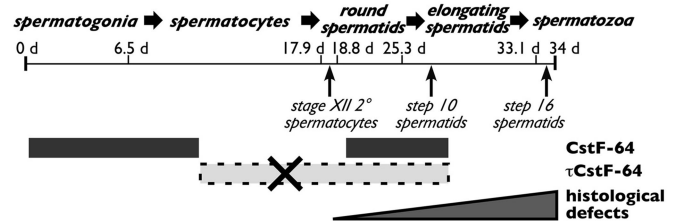
To test that hypothesis, we created *Cstf2t*tm1(Neo) mice containing a targeted deletion of *Cstf2t*, the gene encoding τCstF-64. Here we show that mice homozygous for the *Cstf2t*tm1(Neo) allele (i.e., *Cstf2t*−/−) display aberrant spermatogenesis, resulting in male infertility resembling oligoasthenoteratozoospermia. *Cstf2t*−/− females and *Cstf2t*+/− males and females showed normal fertility. Interestingly, we did not observe a complete block to spermatogenesis in *Cstf2t*−/− mice, as would be expected if τCstF-64 were essential for polyadenylation and subsequent expression of genes during pachynema. Instead, we observed variable expressivity of the *Cstf2t* phenotype, with initial defects visible in secondary spermatocytes and accumulating in number from step-10 spermatids through spermatozoa. In comparing testis mRNA expression by using microarrays, we observed no significant differences between wild-type and *Cstf2t*−/− mice at 17 days postpartum (dpp) but saw significant differences at 22 and 25 dpp. The differences at 22 dpp represented mRNAs encoding proteins involved in basic cellular functions (such as nucleotide metabolism, transcription, splicing, ubiquitination, etc.), whereas the differences at 25 dpp represented spermatogenesis functions, thus explaining the infertility phenotype. These results demonstrate that τCstF-64 is necessary for regulation of gene expression during spermatogenesis and thus necessary for male fertility. This animal model also demonstrates the general importance of mRNA processing in the regulation of essential physiological processes, while providing a model to study
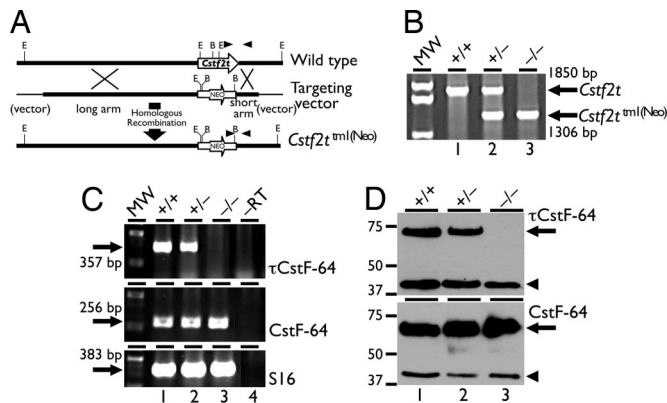
Fig. 2. Targeted disruption of *Cstf2t* eliminates expression of τCstF-64 in testes of *Cstf2t*⁻/⁻ mice. (*A*) Targeted replacement of *Cstf2t* (top line) by a gene-encoding resistance to neomycin (NEO) (bottom line) using homologous recombination in 129SvEv mouse embryonic stem cells. (*B*) Genotyping mice that are wild-type (lane 1, +/+), heterozygous (lane 2, +/−), or homozygous (lane 3, −/−) for the *Cstf2t*^tm1(Neo) allele by genomic PCR. Sizes of fragments from the wild type (*Cstf2t*, 1,850 bp) or mutant (Neo, 1,306 bp) are indicated at the right. (*C*) Expression of τCstF-64 and CstF-64 mRNAs in wild-type (lane 1, +/+), heterozygous mutant (lane 2, +/−), or homozygous mutant (lane 3, −/−) *Cstf2t* mouse testes. Shown is ethidium bromide-stained agarose gel analysis of RT-PCR products from testes of wild-type (lane 1, +/+), heterozygous mutant (lane 2, +/−), or homozygous mutant (lane 3, −/−) *Cstf2t* mice; lane 4 (−RT) is RT-PCR performed but with reverse transcriptase omitted during the cDNA preparation step. Primers pairs were designed to detect τCstF-64 (366 bp) (*Top*), CstF-64 (256 bp) (*Middle*), or ribosomal S16 (382 bp) (*Bottom*) mRNAs. (*D*) Protein immunoblots of testis extracts using antibodies that recognize τCstF-64 [arrow, 70 kDa (*Upper*), 40 μg of protein per lane] or CstF-64 [arrow, 64 kDa (*Lower*), 20 μg of protein per lane] and α-actin [arrowhead, 43 kDa (*Upper* and *Lower*)]. Testis extracts (5) were from either wild-type (lane 1, +/+), heterozygous mutant (lane 2, +/−), or homozygous mutant (lane 3, −/−) *Cstf2t* mice.

polyadenylation in an isolated physiological system that does not affect the viability of the animal. It also shows the essential role of expressed retroposon paralogs of important X-linked genes in the testis.

Results

Cstf2t⁻/⁻ Mice Lack τCstF-64. Mutant mice in which the entire *Cstf2t* coding region was replaced with the neomycin resistance gene NEO1 were produced via homologous recombination [*Cstf2t*^tm1(Neo), Fig. 2*A*]. Homozygous null-*Cstf2t* mice (*Cstf2t*⁻/⁻) were born at the expected Mendelian frequency and showed no obvious effects in viability, life span, size, or overt behavior at any age [supporting information (SI) Fig. 5*A* and data not shown]. Furthermore, there were no differences in sizes or weights of testes, epididymides, or accessory reproductive organs in male mice of any genotype at various stages of postnatal development (SI Fig. 5*B*).

As expected, *Cstf2t*⁻/⁻ mice did not express τCstF-64 mRNA or protein in testes, whereas CstF-64 expression was not significantly affected (Fig. 2 *B–D*).

Male *Cstf2t*⁻/⁻ Mice Are Infertile but Show No Gross Anatomical Differences From Wild-Type Mice. Mating analyses showed that male *Cstf2t*⁻/⁻ mice were infertile and never sired pups (Table 1). In contrast, fertility of female *Cstf2t*⁻/⁻ mice and both male and female *Cstf2t*⁺/⁻ mice were normal (Table 1). Because there were no anatomical differences in reproductive organs among male *Cstf2t*⁺/⁺, *Cstf2t*⁺/⁻, and *Cstf2t*⁻/⁻ mice (SI Fig. 5*B* and Table 2), this suggested that the infertility was not due to major developmental or hormonal blockages in spermatogenesis (14).

Histological examination of seminiferous tubules from adult *Cstf2t*⁻/⁻ mice (Fig. 3 *D–I*) showed a large number of defects at specific stages of spermatogenesis when compared with *Cstf2t*⁺/⁺ mice. There were no apparent defects in premeiotic germ cells, including spermatogonia and pachytene spermatocytes (Fig. 3 *D–J*). Lesions in *Cstf2t*⁻/⁻ tubules were first visible in stage-XII meiotic figures, corresponding with secondary spermatocytes (Fig. 3*F*, see also Fig. 1). Spermiogenesis appeared to proceed normally through step-9 elongating spermatids, with normal acrosome formation and head-shape changes (Fig. 3 *D*, *G*, and *H*).

However, structural defects were clearly visible in step-10 spermatid heads (Fig. 3*I*). These abnormalities increased in number as spermiogenesis progressed, with defects evident such as accumulation of cytoplasmic lobes and residual bodies, fusions of these bodies with the spermatid tails, and abnormal head structures (Fig. 3 *D*, *E*, *G*, and *H*). These varied morphological defects culminated in failure of normal spermiation (15), such that step-16 mature spermatids were present beyond stage VIII (Fig. 3 *D*, *E*, and *H*). Spermiation failure was also manifested as a decrease in the number of spermatozoa seen in the lumen of both *Cstf2t*⁻/⁻ seminiferous tubules (Fig. 3*J*) and epididymides (Fig. 3*K*). These showed very few spermatozoa, most of which were morphologically abnormal, and an unusual preponderance of round spermatids (SI Fig 5*D*) that had sloughed off prematurely into the testicular lumen (Fig. 3*K*). The decreased numbers of epididymal spermatozoa could also be attributed to the loss of germ cells due to abnormal meioses and subsequent reduction in numbers of postmeiotic germ cells.

Variable Expressivity of the *Cstf2t*⁻/⁻ Phenotype in Germ Cells. Interestingly, although many elongating spermatids showed structural defects, not all spermatids were phenotypically alike at the same developmental stage in a given cross-section (compare Fig. 3*D* and Fig. 3*E*). This variability in phenotype might be due to temporal variations in polyadenylation, polyadenylation-induced changes in different transcripts in individual cells, changes in mRNA stability due to differences in lengths of mRNA 3′ untranslated regions, variable expressivity of the polyadenylation defect, or transcript sharing between cells in each cohort (16). Interrupted interactions between germ cells and other testicular cell types, such

Table 1. Fertility of *Cstf2t* mice when mated to CD-1 partners for 4 months

	Genotype		
Gender	+/+	+/−	−/−
Male			
Average litter size ± SD	13.0 ± 0.2 (3)	12.1 ± 2.0 (6)	0 (6)*
Average number of litters ± SD	4.7 ± 0.6	4.8 ± 0.4	0*
Female			
Average litter size ± SD	10.5 ± 0.1 (3)	9.7 ± 1.16 (6)	8.7 ± 1.3 (6)
Average number of litters ± SD	4.7 ± 0.6	4.7 ± 0.8	4.3 ± 0.5

Numbers in parentheses indicate the number of mating pairs. *, $P < 0.001$ (ANOVA test). Comparisons were within each sex across genotypes, but not between sexes.

Table 2. Body and organ weights of 60-dpp male *Cstf2t* mice

Organ	Genotype		
	+/+ (13)	+/− (22)	−/− (11)
Body	24.4 ± 2.35	24.32 ± 2.74	24.79 ± 3.19
Testis	0.088 ± 0.013	0.091 ± 0.018	0.09 ± 0.015
Seminal vesicle	0.18 ± 0.05	0.18 ± 0.04	0.18 ± 0.04
Epididymis	0.027 ± 0.007	0.047 ± 0.027	0.027 ± 0.006

Numbers in parentheses indicate the number of animals. Body and testis weights are in grams ± standard deviation. Other organ weights are in milligrams ± standard deviation. No significant differences were seen between genotypes (ANOVA test).

as Sertoli cells, probably also contributed to the observed variability (15). Together, these data indicate that τCstF-64 affects many spermatogenic processes, possibly via several distinct pathways.

Spermatozoa in *Cstf2t*^{−/−} Males Show a Large Number of Defects Similar to Oligoasthenoteratozoospermia. Examination of cauda epididymal contents showed that *Cstf2t*^{−/−} mice had approximately one-tenth the number of spermatozoa as *Cstf2t*^{+/+} or *Cstf2t*^{+/−} mice (Table 3); this material also contained a large number of unusual round cells (Fig. 3K) that were absent from wild-type mice. In other experiments, we confirmed that the majority of these cells were round spermatids, consistent with a high incidence of premature release of spermatids and other germ cell types (Fig. 3 I and K and SI Fig. 5D). Computer-assisted sperm analysis (CASA) of cauda epididymidal spermatozoa showed that motility and progressivity were significantly reduced in *Cstf2t*^{−/−} mice (Table 3). Note that the vastly reduced number of normal-appearing spermatozoa along with the large number of round cells probably diminished the sensitivity of some parameters determined by CASA. Nevertheless, the few mutant spermatozoa that were motile showed normal curvilinear velocities, amplitudes of lateral head displacement, and flagellar beat frequencies in the range of *Cstf2t*^{+/+} and *Cstf2t*^{+/−} mice (SI Movies 1 and 2). However, these spermatozoa often had other less visible defects in head and tail ultrastructure (data not shown). These defects greatly resembled the human condition of oligoasthenoteratozoospermia, the most common cause of subfertility in men (17). Although the overall effect of loss of *Cstf2t* was male infertility due to low sperm count, the heterogeneity in phenotype of epididymidal spermatozoa is evidence that each germ cell expresses a variable subset of defects that together culminate in the inability to form sufficient numbers of structurally and functionally normal spermatozoa.

***Cstf2t*^{−/−} Males Fail to Fertilize Females.** To test whether the small cohort of morphologically abnormal, albeit motile sperm seen in the cauda epididymides of *Cstf2t*^{−/−} mice were capable of fertilizing wild-type oocytes *in vivo*, we mated *Cstf2t*^{tm1(Neo)} males of all three genotypes with wild-type CD-1 females and compared the numbers of 4-cell, 8-cell, or morula (64-cell and higher) embryos with the numbers of nondividing or degenerate eggs in the oviduct. Vaginal plugs were observed in females after mating with males of all three genotypes, suggesting that mating behavior was not significantly affected by the lack of τCstF-64. However, when embryos were flushed out of the oviducts and examined at 3 days postcoitus (PC), ≈84% of embryos obtained from mating with *Cstf2t*^{+/+} or *Cstf2t*^{+/−} males were at the four-cell, eight-cell, or morula stage (SI Fig. 6 A and B), consistent with normal fertilization. However, none of the oocytes obtained from mating with *Cstf2t*^{−/−} male mice showed signs of normal cleavage (SI Fig. 6 A and C); oocytes obtained from theses matings showed degeneration ranging from remaining at the one-cell stage to granulation and empty ghost-like cells (SI Fig. 6C). Thus, although *Cstf2t*^{−/−} male mice mated normally, the number
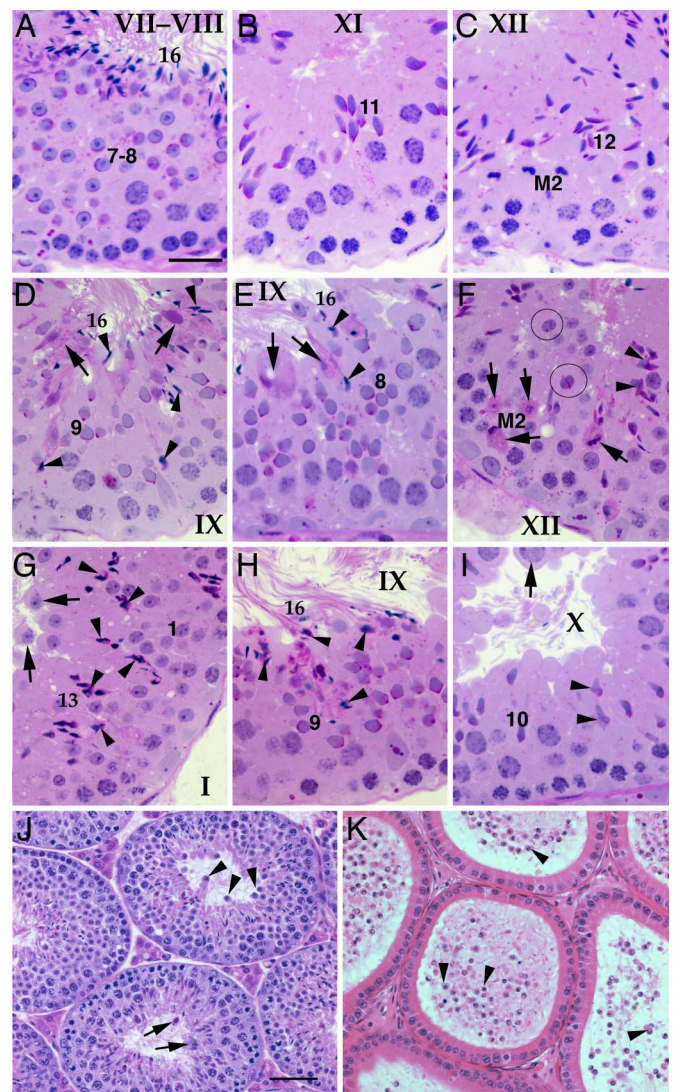

Fig. 3. Lesions in *Cstf2t*^{−/−} mouse testes. (*A–C*) Wild-type testes. Most tubules were normal in appearance, and stages of spermatogenesis consisted of the correct cellular associations. (*A*) Wild-type stage VII–VIII, consisting of step-7–8 and step-16 elongate spermatids (near lumen). (*B*) Wild-type stage XI, with step-11 elongating spermatids. (*C*) Wild-type stage XII with spermatocytes exhibiting condensed chromatin of meiosis 2 and step-12 spermatids. (*D–I*) *Cstf2t*^{−/−} testes. (*D*) *Cstf2t*^{−/−} testis in stage IX, with normal step-9 spermatids but with abnormal retention of step-16 spermatids (arrowheads), indicating failed spermiation. Large abnormal aggregates of residual bodies are seen attached to the retained spermatids (arrows). (*E*) *Cstf2t*^{−/−} testis showing normal step-8 spermatids along with abnormal step-16 spermatids that are not aligning properly for spermiation (arrowheads). Abnormal residual bodies form near the lumen (arrows). (*F*) *Cstf2t*^{−/−} stage XII containing several abnormalities, including degenerative spermatocytes in meiosis 2 (arrows, with PAS+ granulation), binucleate step-1 spermatids (circles), and abnormal elongated spermatid heads (arrowheads). (*G*) *Cstf2t*^{−/−} stage I with normal step-1 spermatids, numerous abnormally shaped step-13 elongated spermatid heads (arrowheads) and evidence of sloughing of round spermatids (arrows). (*H*) *Cstf2t*^{−/−} stage IX, with normal step-9 spermatids but showing abnormal step-16 spermatid heads (arrowheads) being retained within the epithelium. (*I*) *Cstf2t*^{−/−} stage X, with some normal elongating spermatids (10) but also showing early formation of misshapen spermatid heads (arrowheads). Pachytene spermatocytes are also seen near the lumen, where they may be sloughed (arrow). (Scale bar: *A–I*, 25 μm.) (*J*) *Cstf2t*^{−/−} mouse testis at lower magnification to show round spermatids (arrowheads), spermatocytes (arrows), and residual body debris (arrows) being sloughed into the lumen. (Scale bar, 50 μm.) (*K*) *Cstf2t*^{−/−} mouse epididymis showing evidence of extensive sloughing of germ cells and debris by the testis (arrowheads).

Table 3. CASA of cauda epididymal spermatozoa from *Cstf2t* male mice

CASA parameter	Genotype		
	+/+	+/−	−/−
Total sperm (× 10⁶)	17.98 ± 5.98	16.83 ± 1.61	1.74 ± 1.61
Motility	70.4 ± 14.6*	80.6 ± 16.2	6.9 ± 3.8†
Progressivity	67.4 ± 16.2*	78.8 ± 9.4	6.3 ± 3.6†
ALH	11.8 ± 7.8‡	12.3 ± 9.0	7.5 ± 5.6
VCL	227.2 ± 126.6‡	259.8 ± 191.0	142.2 ± 104.3
Linearity	34.1 ± 4.9‡	36.2 ± 3.9	33.0 ± 19.2

Total sperm indicates the total number of spermatozoa per mouse. Motility indicates the percentage of motile spermatozoa. Progressivity indicates the percentage of progressive spermatozoa, ALH, amplitude of lateral head displacement; VCL, curvilinear velocity; Linearity, linear velocity. †, $P < 0.001$ (ANOVA test, Tukey–Kramer multiple comparisons post test). $n = 5$ for each genotype.
*Percent ± SD.
‡Micrometer per second ± SD.

and quality of mature sperm produced appeared to be insufficient to allow fertilization in normal females.

Thousands of mRNAs Are Differentially Expressed in Testes of *Cstf2t*⁻/⁻ Mice. To determine the effects of τCstF-64 on gene expression, we performed microarray analysis on RNA from testes of 17-, 22-, and 25-dpp *Cstf2t*⁺/⁺ and *Cstf2t*⁻/⁻ mice by using the Affymetrix GeneChip Mouse Expression Set 430 (version 2.0). These ages were chosen because they span the times at which pachytene spermatocytes and early spermatids become prominent during the first round of spermatogenesis (18). Using the significance analysis of microarray (SAM) tool, we did not find any differentially expressed genes between *Cstf2t*⁺/⁺ and *Cstf2t*⁻/⁻ mice at 17 dpp (Fig. 4A), suggesting that τCstF-64 does not have significant effects at that early time. In contrast, 4,692 genes (6,367 probe sets) were expressed differentially at 22 dpp, representing 22.9% of genes detectable at this stage of development (SI Table 4). Interestingly, fewer genes (3,061 genes; 3,922 probe sets) were expressed differentially at 25 dpp (SI Table 5), suggesting a greater impact of *Cstf2t*⁻/⁻ at 22 dpp than at 25 dpp. However, the genes selected in the 25-dpp comparison tended to have larger magnitude changes than those at 22 dpp [indicated by the slopes of lines for observed score versus expected score (Fig. 4A) and by distribution of differentially expressed genes in different fold change ranges (SI Tables 4 and 5)]. In addition, genes selected in the 22-dpp comparison did not greatly overlap with those at 25 dpp (Fig. 4B), and more down-regulated genes than up-regulated genes were found for 22 dpp than at 25 dpp.

We examined the incidence of alternative polyadenylation for up- and down-regulated genes at 22 dpp and 25 dpp by comparison with PolyA_DB 2 (19) and found that up-regulated genes at 22 dpp tended to have a single polyadenylation site, and down-regulated genes tended to have alternative sites; the opposite trends were observed at 25 dpp (SI Fig. 7). Similarly, we examined potential RNA regulatory elements, including AAUAAA, U-rich, and UG-rich elements (20). None of these elements were significantly associated with up- or down-regulated genes at 22 or 25 dpp except upstream U-rich elements. These elements showed a slightly higher representation in down-regulated genes at 22 dpp and in up-regulated genes at 25 dpp (SI Fig. 7).

We conducted cluster analyses for genes that were differentially expressed in 22- or 25-dpp samples (Fig. 4C). Samples from 17 dpp *Cstf2t*⁺/⁺ and *Cstf2t*⁻/⁻ mice clustered very closely, indicating that gene-expression profiles in these two samples were very similar. As expected, samples from *Cstf2t*⁺/⁺ and *Cstf2t*⁻/⁻ could be distin-
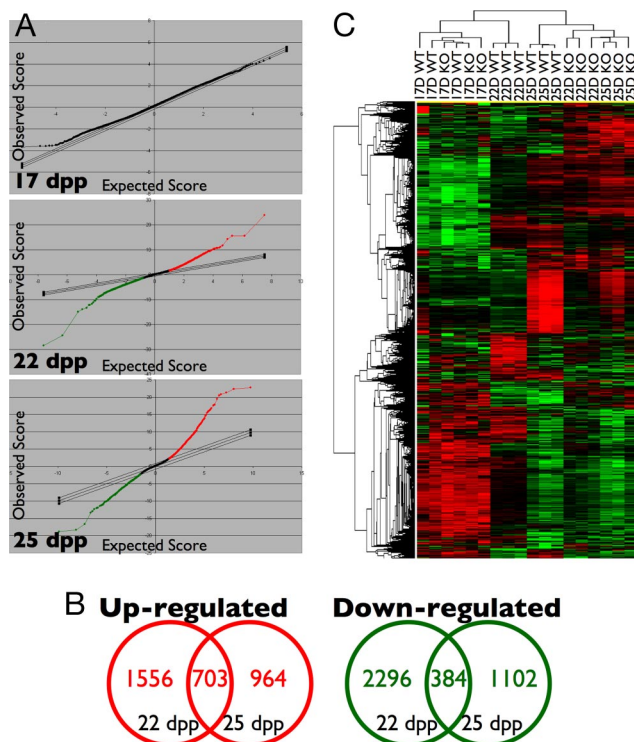

Fig. 4. Microarray analyses. (A) Differentially expressed genes between wild-type and *Cstf2t*⁻/⁻ mouse testes. SAM plots are shown for various time points of development (17, 22, and 25 dpp). Each dot is a probe set corresponding to differentially expressed genes, with red dots being up-regulated and green dots being down-regulated genes in knockout samples. (B) Venn diagram showing relationships of significantly changed genes in 22 and 25 dpp samples. (C) Hierarchical clustering performed using 8,913 probe sets selected by SAM and constructed by Pearson correlation and average linkage. Expression values for each probe set across all samples were median-centered and normalized, with red indicating values above and green indicating values below the median.

guished readily at both 22 and 25 dpp, indicating significantly different gene expression between the two genotypes at both time points. Interestingly, gene expression profiles of 22- and 25-dpp *Cstf2t*⁻/⁻ samples were more similar to one another than to their respective wild-type samples, suggesting that the gene expression program in *Cstf2t*⁻/⁻ does not progress as the wild type does.

Finally, we examined gene ontology (GO) terms for genes selected by the 22- and 25-dpp comparisons to find common functional pathways for selected genes. A greater number of GO terms were significantly associated with genes selected by the 22-dpp comparison than the 25-dpp comparison (SI Table 6). Genes selected by the 22-dpp comparison were associated with general functions, such as RNA metabolic processes, RNA transcription, splicing, ubiquitination, and others (GO:0016070, GO:0019219, GO:0006512, etc.), although reproductive processes were also affected (GO:0019953, GO:0019861, etc.). However, genes selected by the 25-dpp comparison were associated with spermatogenesis and male gamete formation (GO:0019953, GO:0007283, GO:0048232, etc.), consistent with the developmental progression of spermatogenic defects observed in the *Cstf2t*⁻/⁻ mice and reflected in their infertility.

Discussion

Alternative mRNA splicing (21) and polyadenylation (3, 4) significantly increase diversity of gene expression in male germ cells. τCstF-64 is a candidate for controlling polyadenylation in male germ cells (8). We hypothesized that τCstF-64 would be essential

Dass *et al.*

DEVELOPMENTAL BIOLOGY

www.manaraa.com

for spermatogenesis and male fertility because of its expression during male meiosis when CstF-64 is absent (5). In support of this hypothesis, $Cstf2t^{-/-}$ males were infertile due to low sperm counts (Table 3), significant developmental defects in spermiogenesis (Fig. 3), and structurally abnormal spermatozoa (SI Fig. 5D). Furthermore, $Cstf2t^{-/-}$ females showed normal fertility, indicating that τCstF-64 played little or no role in female fertility. We observed no gross differences in size or weight of male reproductive organs (SI Fig. 5B and Table 2), although there were significant abnormalities in epididymal sperm (Fig. 3 I and K and Table 3), conditions that match human oligoasthenoteratozoospermia (17). Consistent with this condition, $Cstf2t^{-/-}$ males failed to impregnate wild-type females (SI Fig. 6 and Table 1). We did not observe effects on other organs (Table 2 and SI Fig. 5 A and B) or overt neurological or immunological effects, suggesting that the major physiological processes affected by τCstF-64 were limited to spermatogenesis.

Within the seminiferous epithelia of $Cstf2t^{-/-}$ mice, no defects were visible in spermatogonia or spermatocytes through diplonema; defects were first visible in secondary spermatocytes as abnormal meiotic figures (Fig. 3F and SI Fig. 6). Although we have not eliminated the possibility that molecular lesions occurred in earlier cell types, this suggests that some of the earliest defects due to lack of τCstF-64 were in chromatid segregation during meiosis II. Expression of a number of genes involved with microtubule motors and chromosome dynamics were altered in $Cstf2t^{-/-}$ testis at 22 dpp (SI Table 4), which could contribute to the phenotype. We also saw considerable morphological defects in flagellar microtubule structures in epididymal spermatozoa (data not shown), which could be a later reflection of these same issues.

Microarray results indicated that τCstF-64 was important for the correct expression of thousands of mRNAs expressed during male germ cell development, becoming critical between 17 and 22 dpp (Fig. 4A). The importance of τCstF-64 in spermatogenesis was established at 25 dpp, because genes showing greatest change in their expression at this time were associated with spermatogenesis (SI Table 5). Furthermore, expression of a large number of genes was affected by ablation of τCstF-64, resulting in mRNAs that both increased and decreased in abundance (SI Tables 4 and 5). In examining these genes, several points stand out. First, we did not observe a majority of down-regulated mRNAs. This would be expected if loss of τCstF-64 led solely to down-regulation of gene expression due to an overall decrease in 3′ end processing. Next, GO term analysis showed that functions of affected genes changed from general functions in gene expression at 22 dpp to more specific functions in spermatogenesis at 25 dpp (SI Table 6). Third, we did not observe an association of any specific RNA element with genes at 22 or 25 dpp that could support a direct effect of τCstF-64 on expression of these genes (SI Fig. 7).

These data suggest that more than one mechanism is affecting gene expression in testes of $Cstf2t^{-/-}$ mice, leading us to propose the following hypothesis: a limited number of genes are affected directly by loss of τCstF-64; we designate these genes "primary targets." Other genes that are affected by changes in expression of those primary targets are therefore "secondary targets." We propose further that a small number of primary target genes are affected by loss of τCstF-64 between 17 and 22 dpp and that a larger number of the genes affected at later times are secondary targets.

In support of this hypothesis, ablation of τCstF-64 resulted in decreased expression of transcriptional and posttranscriptional regulatory genes at 22 dpp (SI Table 4). Clearly, decreases in those gene products could have positive and negative effects on the expression of a large number of secondary gene products, such as those observed at 25 dpp (SI Table 5). Furthermore, we observed variable expressivity of τCstF-64 in the $Cstf2t^{-/-}$ mice and cumulative defects in testes of these mice (Fig. 3). This observation is consistent with loss of τCstF-64 resulting in a cascade of varying secondary effects.

How might loss of τCstF-64 affect expression of primary target genes? Most directly, in some genes, absence of τCstF-64 would lead to deficient 3′ end formation and loss of expression. However, in other genes, altered polyadenylation site choice would result in changes in 3′ untranslated regions, leading to altered mRNA stability. Future experiments will attempt to differentiate the affected genes into classes based on these potential mechanisms.

In addition to its proposed role in cotranscriptional control of gene expression, τCstF-64 is an example of the class of testis-enriched, expressed retroposed genes that are paralogs of important X-linked genes (22–24). Because MSCI leads to inactivation of a number of essential X-linked genes, retroposed paralogs have taken on significant functions in male meiosis. Mutation or deletion of most (25–28), but not all (29) of these expressed retroposons lead to male infertility but to few other physiological defects. Because loss of $Cstf2t$ leads to highly specific effects on male fertility, we believe it supports the argument that a large number of these retroposed paralogs arose for reproductive purposes, likely at the time the heteromorphic system of sex determination arose in mammals (30), ≈310 million years ago (31, 32).

Unexpectedly, we observed no morphological defects in pachytene spermatocytes in $Cstf2t^{-/-}$ mice and no differentially expressed genes at 17 dpp, when pachytene spermatocytes comprise 27–36% of total cells in the seminiferous epithelium (18). This observation was surprising because τCstF-64 is normally expressed in pachynema, when CstF-64 is absent (5, 12), and therefore would be expected to have a profound effect on gene expression. We are compelled to ask how mRNA expression and polyadenylation is enabled in these cells in the absence of CstF-64 and τCstF-64. Possible mechanisms include undetectably low residual CstF-64 protein in these cells that can compensate for the lack of τCstF-64, the presence of a hitherto undetected protein that functions in place of CstF-64 in pachynema, a reduced meiotic requirement for CstF-64 or its homologs, or delayed effects of alterations in τCstF-64-dependent gene products until later stages of spermatogenesis. $Cstf2t^{-/-}$ mice will provide us with tools to test these and other interesting hypotheses.

Materials

Generation of $Cstf2t^{tm1(Neo)}$ Mice by Homologous Recombination. A targeting vector was created using the $Cstf2t$ coding region from chromosome 19 (33) with pGK-Neo (Fig. 2A), electroporated into 129SvEv ES cells, G418-resistant colonies were selected, and colonies in which Neo had replaced $Cstf2t$ were identified by PCR. ES cells were microinjected into C57BL/6 embryos and reimplanted into pseudopregnant females. Mice that displayed a high degree of chimerism were identified and bred to wild-type C57BL/6 mice to generate F$_1$ progeny. Germ-line transmission was confirmed by PCR analysis of F$_1$ animals (Fig. 2 A and B). Subsequent animal studies were performed at Texas Tech University Health Sciences Center, in accordance with protocols according to National Institutes of Health guidelines, and approved by the Institutional Animal Care and Use Committee. $Cstf2t^{tm1(Neo)}$ mice used in these studies were of mixed C57BL/6–129SvEv background. CD-1 outbred mice used in the mating analysis were purchased from Charles River Laboratories.

Genotyping of $Cstf2t^{tm1(Neo)}$ Mice by PCR. Genomic DNA was extracted from tail snips of $Cstf2t^{tm1(Neo)}$ mice by proteinase K digestion, followed by ethanol precipitation. PCRs were performed using $Cstf2t$- and $Cstf2t^{tm1(Neo)}$-specific primers to determine the presence of the transgene (Fig. 2B).

RNA Analysis. Total RNA was extracted from the testes of $Cstf2t^{tm1(Neo)}$ mice by using TRIzol reagent (Invitrogen), treated with DNase (Ambion), and 2.0 μg was used to synthesize oligo(dT)-primed first-strand cDNA by using SuperScript II Reverse Transcriptase (Invitrogen). PCRs using τCstF-64-specific primers were performed using the Idaho Technology Air Thermocycler, and products were separated via ethidium bromide-stained TAE gels.

Protein Analysis. Testes were dissected from 60-dpp $Cstf2t^{tm1(Neo)}$ mice, decapsulated, washed several times in PBS containing 1 mM PMSF to remove interstitial cells, sonicated, and boiled in SDS loading buffer (34). Total protein concentration

was measured using the Bradford assay (BioRad), and 20 or 40 μg of total protein separated by SDS/10% PAGE was immunoblotted using 3A7 (1:50) and 6A9 (1:25) anti-CstF-64 monoclonal antibodies, respectively (5). A mouse monoclonal antibody against α-actin (1:2,000; Chemicon MAB1501R) was used for comparison of loading.

Animal Studies. Male mice were euthanized at 43, 60, 85, and 108 dpp, the intact body was weighed and dissected, and weights were obtained for each testis, epididymis, and seminal vesicle. Statistical comparisons of the weights (ANOVA) were performed using GraphPad InStat software.

Mating Analyses. Adult (43–96 dpp) male and female $Cstf2t^{+/+}$, $Cstf2t^{+/-}$, and $Cstf2t^{-/-}$ mice were housed individually with an 8-week-old CD-1 mouse of the opposite sex. Total number of pups per litter, sex ratio and genotype of pups per litter, and total number of litters were collected over a 4-month interval. Statistical analysis and ANOVA were performed using Microsoft Excel and GraphPad InStat software.

Histology. Adult male $Cstf2t^{tm1(Neo)}$ mice were given 5 units of heparin i.p. 15 min before ketamine anesthetization, followed by cardiac perfusion with Ringer's bicarbonate (pH 7.4) containing 0.5% wt/vol procaine (Acros Organics) at 110 ml/min for 2 min, followed by 4% glutaraldehyde (Electron Microscopy Sciences) in 0.085 M phosphate buffer at 110 ml/min for 2–4 min, followed by 10 ml/min for 20–30 min. Testes were dissected and incubated overnight at 4°C in fixative, followed by embedding in glycol methacrylate Technovit 7100 (Energy Beam Sciences). Sections (2.5 μm) were stained with hematoxylin and periodic acid–Schiff for histological analysis (15).

CASA. Cauda epididymides from 110-dpp $Cstf2t^{+/+}$, $Cstf2t^{+/-}$, and $Cstf2t^{-/-}$ mice were minced at 37°C in modified Tyrode's medium [5% CO_2 (pH 7.4)] supplemented with 1.8 mM $CaCl_2$, 0.4% BSA, and 0.5 mM pyruvate before use and incubated for 10 min at 37°C in 5% CO_2 to release spermatozoa. Cell concentration was adjusted to 8 million/ml, and CASA was performed using the Hamilton

Thorne Biosciences Ceros system on an Olympus CX-41 microscope fitted with a CCD camera and Minitherm slide warmer (35). Sperm cell tracks were captured in an 80-μm chamber at 60 Hz. Ten arbitrary and independent fields were captured for four male mice of each genotype, analyzing 60–100 spermatozoa per field. Video of the spermatozoa was captured using the same system.

In Vivo Oocyte Fertilization. CD-1 female mice (8 weeks or older) were mated with $Cstf2t^{+/+}$, $Cstf2t^{+/-}$, or $Cstf2t^{-/-}$ male mice and inspected daily for the presence of vaginal plugs (day 1 PC). At this time, the female was separated from the male. On day 3 PC, females were euthanized, and oviducts were dissected into PBS. Each oviduct was flushed with PBS by using a 50-μl pulled micropipette, and cumulus cells were removed into PBS by pipetting to wash. Oocytes were observed for cleavage activity by using an Olympus BX-60 photomicroscope. Embryos were scored as 4-cell, eight-cell, or morula stage, whereas unfertilized oocytes were scored as undivided single cells, granular cells, or ghost or empty cells.

Microarray Data Analysis. Raw intensity values were normalized across all arrays by using the robust multiarray analysis (RMA) method, and probe sets with detectable fluorescence signals were determined by the MAS 5.0 algorithm (36, 37). Differentially expressed genes in wild-type and knockout mice were identified by SAM using 5% FDR and fold change >1.2 (38). GO entries were evaluated for their association with differentially expressed genes by using the hypergeometric distribution test (39). P values were adjusted for multiple testing errors (40). Hierarchical cluster analysis was performed in Cluster 3.0 and visualized by the TreeView program (41).

1. Edmonds M (2002) *Prog Nucl Acid Res Mol Biol* 71:285–389.
2. Zhao J, Hyman L, Moore C (1999) *Microbiol Mol Biol Rev* 63:405–445.
3. Edwalds-Gilbert G, Veraldi KL, Milcarek C (1997) *Nucleic Acids Res* 25:2547–2561.
4. Zhang H, Lee JY, Tian B (2005) *Genome Biol* 6:R100.
5. Wallace AM, Dass B, Ravnik SE, Tonk V, Jenkins NA, Gilbert DJ, Copeland NG, MacDonald CC (1999) *Proc Natl Acad Sci USA* 96:6763–6768.
6. MacDonald CC, Redondo, JL (2002) *Mol Cell Endocrinol* 190:1–8.
7. Liu D, Brockman JM, Dass B, Hutchins LN, Singh P, McCarrey JR, MacDonald CC, Graber JH (2007) *Nucleic Acids Res* 35:234–246.
8. Dass B, McMahon KW, Jenkins NA, Gilbert DJ, Copeland NG, MacDonald CC (2001) *J Biol Chem* 276:8044–8050.
9. Wilusz J, Shenk T (1988) *Cell* 52:221–228.
10. Moore CL, Chen J, Whorisky J (1988) *EMBO J* 7:3159–3169.
11. Takagaki Y, Manley JL, MacDonald CC, Wilusz J, Shenk T (1990) *Genes Dev* 4:2112–2120.
12. Wallace AM, Denison T, Attaya EN, MacDonald CC (2004) *Biol Reprod* 70:1080–1087.
13. Handel MA (2004) *Exp Cell Res* 296:57–63.
14. Kumar TR (2005) *Reproduction* 130:293–302.
15. Russell LD, Ettlin RA, Sinha Hikim AP, Clegg ED (1990) *Histological and Histopathological Evaluation of the Testis* (Cache River Press, Clearwater, FL).
16. Peschon JJ, Behringer RR, Brinster RL, Palmiter RD (1987) *Proc Natl Acad Sci USA* 84:5316–5319.
17. Hirsh A (2003) *BMJ* 327:669–672.
18. Bellvé, AR (1993) *Methods Enzymol* 225:84–113.
19. Lee JY, Yeh I, Park JY, Tian B (2007) *Nucleic Acids Res* 35:D165–D168.
20. Hu J, Lutz CS, Wilusz J, Tian B (2005) *RNA* 11:1485–1493.
21. Venables JP (2002) *Curr Opin Genet Dev* 12:615–619.
22. Wang PJ, McCarrey JR, Yang F, Page DC (2001) *Nature Gen* 27:422–426.
23. Wang PJ, Page DC, McCarrey JR (2005) *Hum Mol Gen* 14:2911–2918.
24. Emerson JJ, Kaessmann H, Betran E, Long M (2004) *Science* 303:537–540.
25. Rohozinski J, Bishop CE (2004) *Proc Natl Acad Sci USA* 101:11695–11700.
26. Bradley J, Baltus A, Skaletsky H, Royce-Tolland M, Dewar K, Page DC (2004) *Nat Genet* 36:872–876.
27. Wang PJ, Page DC (2002) *Hum Mol Gen* 11:2341–2346.
28. Cheng Y, Buffone MG, Kouadio M, Goodheart M, Page DC, Gerton GL, Davidson I, Wang PJ (2007) *Mol Cell Biol* 27:2582–2589.
29. Banks KG, Johnson KA, Lerner CP, Mahaffey CL, Bronson RT, Simpson EM (2003) *Genomics* 82:254–260.
30. Ohno S (1967) *Sex Chromosomes and Sex-Linked Genes* (Springer, New York).
31. Hedges SB, Kumar S (2004) *Trends Genet* 20:242–247.
32. Lahn BT, Page DC (1999) *Science* 286:964–967.
33. Osoegawa K, Tateno M, Woon PY, Frengen E, Mammoser AG, Catanese JJ, Hayashizaki Y, de Jong PJ (2000) *Genome Res* 10:116–128.
34. Laemmli UK (1970) *Nature* 227:680–685.
35. Quill TA, Sugden SA, Rossi KL, Doolittle LK, Hammer RE, Garbers DL (2003) *Proc Natl Acad Sci USA* 100:14869–14874.
36. Affymetrix (2006) *Affymetrix Expression Console Software Version 1.0: User Guide* (Affymetrix, Inc., Santa Clara, CA).
37. Irizarry RA, Hobbs B, Collin F, Beazer-Barclay YD, Antonellis KJ, Scherf U, Speed TP (2003) *Biostatistics* 4:249–264.
38. Tusher VG, Tibshirani R, Chu G (2001) *Proc Natl Acad Sci USA* 98:5116–5121.
39. Rivals I, Personnaz L, Taing L, Potier MC (2007) *Bioinformatics* 23:401–407.
40. Benjamini Y, Drai D, Elmer G, Kafkafi N, Golani I (2001) *Behav Brain Res* 125:279–284.
41. Eisen MB, Spellman PT, Brown PO, Botstein D (1998) *Proc Natl Acad Sci USA* 95:14863–14868.

DEVELOPMENTAL BIOLOGY

Dass *et al.*

www.manaraa.com